Phase Synchronization for Non-Binary Coded CCSK Short Frames

Kassem Saied, Ali Al Ghouwayel, Emmanuel Boutillon

Phase Synchronization for Non-Binary Coded CCSK Short Frames

Kassem Saied
Lab-STICC (UMR 6285)
Université Bretagne Sud,
Lorient, France
Lebanese International University,
Beirut, Lebanon
Kassem.saied@univ-ubs.fr

Ali Chamas Al Ghouwayel
Lebanese International University,
Beirut, Lebanon
EFREI, Paris, France
ali.ghouwayel@efrei.fr

Emmanuel Boutillon
Lab-STICC (UMR 6285)
Université Bretagne Sud
Lorient, France
Emmanuel.boutillon@univ-ubs.fr

***Abstract*—This paper proposes a phase and frequency synchronization technique in the context of Cyclic Code Shift Keying (CCSK) modulation associated with Non-Binary Low Density Parity Check Matrix (NB-LDPC) codes. Two methods are proposed. The first, called Direct Method (DM), is a direct estimation of the parameters of a noisy sinusoidal. The second, called Parametric Method (PM), is based on the Maximum Likelihood estimation using a distribution parameterized by the CCSK demodulator and the NB-LDPC decoder. The Frame Error Correction (FEC) results show that the performance of the proposed phase synchronized frame approximately maintains the same performance as when a Genius-Aided estimation is used, or when no phase offset exists. This is achieved at a very low Signal to Noise Ratio (SNR) around -10 dB.**

***Index Terms*—Phase synchronization, ML estimator, CCSK score ratio, NB-code properties.**

I. Introduction

The design of an efficient signaling scheme for the Internet of Things (IoT) systems constitutes nowadays an active research domain [1]. Being the center of interest for both academic and industrial sectors, the infrastructure of IoT systems is needed to be adapted to support massive connections induced by the overgrowing number of users [2]. In this context, the frame structure of an IoT Packet constitutes one of the aspects to be appropriately designed. The target is to shorten this frame as long as the communication quality predefined by the standard is maintained at the required level [3]. This frame shortening strategy is motivated by the work of Polyanski [4] where it was demonstrated that the capacity of the wireless channel is not affected by the asynchronous transmission, even when short packets are used. In the context of IoT communications, the challenge is to propose techniques able to maintain good performance at very low Signal to Noise Ratio (SNR) levels.

Time, phase, and frequency synchronizations for a short frame are topics widely investigated in the literature. They can be splitted into two areas: data-assisted synchronization (thanks to the preamble and/or pilot symbols) and blind synchronization. The literature for the latter case is rather sparse. Most of the proposed methods work only for a rather high signal-to-noise (SNR) ratio [5]–[7]. In [8], a phase synchronization method has been proposed based on the use of turbo decoder information to improve the carrier phase and offset synchronization for short packets. This method showed good performance at an SNR greater than -0.5 dB.

In [9], a Quasi Cyclic Short Packet (QCSP) frame structure has been proposed based on the combinations of Cyclic Code Shift Keying (CCSK) [10] of length q chips and a Non-Binary (NB) error control code [11] over GF(q). The key idea is to design a preamble-less frame, where the whole payload is used to perform both detection and timing synchronization processes from the first side, and Forward Error Correction (FEC) decoding process to recover the conveyed data from the other side. The detection and time-synchronization techniques are successfully and efficiently performed thanks to the inherent cyclic property of the CCSK modulation, allowing practical transmission at very low SNR (-10 dB for example). In [12], a robust detection method to assess the arrival of a QCSP frame is presented. This method called "time sliding method", provides only a rough estimate of the time of arrival of the frame as well as a rough estimate of its frequency offset. In [13], an efficient time synchronization technique is described. The method uses the structural properties of the QCSP frame to detect the exact time of arrival of the frame.
In the continuity of the workflow initiated in [9], [12] and [13], this paper presents the final step of the synchronization process, i.e., the suppression of the remaining residual frequency and initial phase offsets. Once the frame fully synchronized, coherent demodulation can be performed to generate the symbol Log-Likelihood Ratio required by the non-binary decoder.

In this paper, two methods are proposed to perform phase/frequency synchronization. The first method, called Direct Method (DM), assumes that all the CCSK symbols are demodulated correctly. In that case, the frequency and phase estimation task resumes to an estimation problem of a pure complex sinusoidal signal affected by Gaussian noise. It is a well-known problem and a near Maximum Likelihood (ML) estimator can be obtained at low cost using the Fast Fourier

This work has been partly funded by the French ANR under grant number ANR-19-CE25-0013-01 (QCSP Project: https://qcsp.univ-ubs.fr/).

Transform (FFT) [14]. Nevertheless, at low SNR (-10 dB typically), detection errors appear. Those errors alleviate the quality of the DM and generate up to 0.5 dB of degradation on the overall performance. The second method is called Parametric Method (PM). It is based on the ML estimation using a parametric Probability Density Function (PDF) of each phase error. The two parameters of the proposed PDF model are computed using information coming from the non-coherent CCSK demodulation process and information coming from one decoding iteration of the NB-Low Density Parity Check (NB-LDPC) decoder. The PM method is simple to process and gives a result close to the Genius Aided (GA) method, i.e., the DM method when all the transmitted symbols are considered to be known.

The rest of this article is organized in the following manner. In section II, the general context of our study including the system model and the problem statement of the phase synchronization are discussed. In section III, the direct phase synchronization method is described. The proposed PM phase synchronization aided by the CCSK and NB-LDPC association is described in Section IV. Discussion and result analysis are given in section IV. Finally, section V concludes and gives some insights on future work.

II. General Context of the Study

This section sums up briefly the overall communication chain of the QCSP system model. Then, it states the problem of phase synchronization and formulates the context of the proposed phase-synchronization algorithm.

A. Overall Communication Chain

Fig. 1 shows the system model of the communication link being considered, where the phase-synchronization and LLR computation block constituting the core contribution of this work is highlighted.

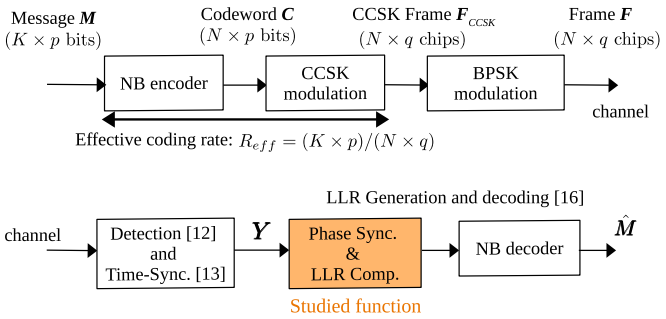

Fig. 1. Overall Communication Principle.

Consider a NB code defined over the Galois Field with q elements, denoted by GF(q), i.e., $q = 2^p$. A message $\boldsymbol{M}$ consists of K GF(q) information symbols, each symbol of size p bits. It is encoded by the NB-LDPC code of Parity Check Matrix (PCM) $\boldsymbol{H}$ and code rate $R_c = K/N$, where N is the length of the generated codeword $\boldsymbol{C}$, i.e. $\boldsymbol{C} = [c_0, c_1, \ldots, c_{N-1}]$. Thus, the codeword $\boldsymbol{C}$ verifies $\boldsymbol{H}\boldsymbol{C}^T = 0$, where $\boldsymbol{C}^T$ is the transpose of $\boldsymbol{C}$. The CCSK modulation uses a pseudo-random binary sequence $\boldsymbol{P}_0 = \{P_0(i)\}_{i=0,\ldots,q-1}$ of length q, where $P_0(i) \in \{-1, 1\}$, to map an element c_k of GF(q) (c_k can also be considered as an integer between 0 and $q-1$) to the sequence $\boldsymbol{P}_{c_k}$ defined as the circular right shift of $\boldsymbol{P}_0$ by c_k positions, i.e., $\boldsymbol{P}_{c_k} = \{P_0(i - c_k \bmod q)\}_{i=0,\ldots,q-1}$ for $k \in [0, N-1]$. The CCSK sequence P_0 is selected so that the scalar product $< P_a, P_b >$ is close to 0 when $a \neq b$ and equal to q otherwise (see [15] for the definition of the sequences P_0 for several values of q). So the QCSP frame $\boldsymbol{F}$ can be defined as: $\boldsymbol{F} = [\boldsymbol{P}_{c_0}, \boldsymbol{P}_{c_1}, \ldots, \boldsymbol{P}_{c_{N-1}}]$. Before transmission, the generated frame $\boldsymbol{F}$ is composed of $N \times q$ BPSK symbols, which are then shaped by a half raised cosine filter with a roll-off factor equal to 0.35.

The QCSP frame passes through an asynchronous Additive White Gaussian Noise (AWGN) channel with a standard deviation σ. Since an unslotted ALOHA protocol is assumed, the receiver has no knowledge about the time of arrival of the frame, its potential residual frequency offset, and finally, its initial phase offset. In [12], a detection technique named "time sliding windows" allows determining the arrival of a frame with high probability. Then, in [13], a time-synchronization method is proposed to mitigate the time ambiguity and to suppress most of the frequency offset. The output of the detection and time-synchronization processes (see Fig. 1) is thus the received frame affected by a small residual frequency offset f_r upper bounded by 10^{-3}, i.e. the absolute phase offset between two chips is lower than $2\pi \times 10^{-3}$ radian [13]. The model of the frame sent to the phase synchronization block is thus defined as $\boldsymbol{Y} = [\boldsymbol{y}_0, \boldsymbol{y}_1, ..., \boldsymbol{y}_{N-1}]$, where $\boldsymbol{y}_k = (y(kq), y(kq+1), \ldots, y(kq+q-1))$, corresponds to the transmission of the sequence $\boldsymbol{P}_{c_k}$ affected by phase rotation and corrupted by additive Gaussian noise, i.e. for $k = 0, 1, ..., N-1$, and $\ell \in 0, 1, ..., q-1$.

$$y_k(\ell) = e^{j(2\pi f_r(kq+\ell)+\phi_0)} P_{c_k}(\ell) + z(qk+\ell). \quad (1)$$

The contribution of the paper is to explain how the phase synchronization blocks mitigates both f_r and ϕ_0.

B. Problem statement

Assuming perfect frequency synchronization, the generation of the Log Likelihood vectors required by the NB-LDPC decoder is based on computation that uses the real part of the output correlation vector $\boldsymbol{L}$ (see [16] for details). Let us assume that a residual phase error ξ affects the correlation vector $\boldsymbol{L}$. The real part of $\boldsymbol{L}$ will have an amplitude reduced by a factor $\cos(\xi)$ compared to the magnitude $|\boldsymbol{L}|$ due to the rotation by the angle ξ. This amplitude degradation translates directly in $10\log_{10}(\cos(\xi)^2)$ dB loss of signal energy, and thus, the SNR. To set the idea, $\xi = 0, \pi/64, \pi/16, \pi/9.3$ and $\pi/4$ generates an SNR degradation of 0 dB, 0.01 dB, 0.16 dB, 0.5 dB and 3 dB, respectively. When $\xi = \pi/2$, no more signal is received. The frequency synchronization task should thus maintain the residual phase error close to zero not to impact significantly the receiver performance.

C. Demodulation of the received symbol

The first step is to demodulate each symbol. Let us define $\boldsymbol{L}_k = \{L_k(i)\}_{i=0,1,...,q-1}$ as the correlation vector between the vector $\boldsymbol{y}_k$ and the q possible CCSK sequences $\boldsymbol{P}_i$ for $i = 0, 1, ..., q-1$, i.e.

$$L_k(i) = \sum_{\ell=0}^{q-1} y_k(\ell) P_i(\ell). \tag{2}$$

By definition of (2) and (1), we have

$$\begin{aligned} L_k(c_k) &= e^{j(2\pi f_r k q + \phi_0)} \sum_{\ell=0}^{q-1} e^{j2\pi f_r \ell} P_{c_k}(\ell)^2 + \sum_{\ell=0}^{q-1} z(qk+\ell) P_{c_k}(\ell) \\ &= e^{j(2\pi f_r k q + \phi_0)} \frac{1 - e^{j2\pi f_r q}}{1 - e^{j2\pi f_r}} + Z_k, \\ &= e^{j(\omega k + \theta)} \frac{\sin(\pi f_r q)}{\sin(\pi f_r)} + Z_k, \end{aligned} \tag{3}$$

where $\omega = 2\pi f_r q$, $\theta = \phi_0 + \pi f_r (q-1)$ and Z_k the summation of q independent samples of an AWGN noise of standard deviation equal to σ, i.e., Z_q is Gaussian noise with zero mean and standard deviation $\sqrt{q}\sigma$. In the absence of noise (i.e. $Z_k = 0$), the phase of $L_k(c_k)$ is equal to $\Theta_k = \omega_k + \theta$. Note that Θ_k is the equation of a straight line in the phase domain, as shown in the black solid line of Fig. 2.

Let d_k be the symbol hard decision of the non-coherent demodulation process, so d_k is defined as

$$d_k = \underset{i=0,1,...,q-1}{\operatorname{argmax}} \{|L_k(i)|\}. \tag{4}$$

From d_k, the corresponding correlation value can be defined as

$$\gamma_k = L_k(d_k). \tag{5}$$

Thus, in case of correct decision, i.e., when $d_k = c_k$, γ_k is equal to $L_k(c_k)$ given in (3). In case of wrong decision, we have

$$\gamma_k = e^{j(\omega k + \phi_0)} \sum_{\ell=0}^{q-1} e^{j2\pi f_r \ell} P_{c_k}(\ell) P_{d_k}(\ell) + Z_k. \tag{6}$$

Since by construction, $< P_{d_k}, P_{c_k} >$ is close to zero and considering also that $|q f_r| \ll 1$ (a reasonable assumption for $q = 64$ and $|f_r| < 10^{-3}$), then the first term of (6) can be considered as negligible. In that case, γ_k has a random phase given by the phase of the noise term Z_k of (6).

Let $\boldsymbol{\Gamma}$ denotes the vector containing the γ_k values found in (5), i.e., $\boldsymbol{\Gamma} = (\gamma_k)_{k=0,1,...,N-1}$. Let us define $\boldsymbol{\Psi} = (\Psi_k)_{k=0,1,...,N-1}$, where Ψ_k is the phase of γ_k for $k \in 0, 1, \ldots, N-1$. We can notice from (3) that Ψ_k is modeled as

$$\Psi_k = \Theta_k + \xi_k, \tag{7}$$

with ξ_k is the phase error between the exact phase Θ_k of $L_k(c_k)$ in the absence of noise and the measured phase Ψ_k of $L_k(d_k)$. Fig. 2 illustrates with an example the impact of the channel on the phase of $N = 60$ detected symbols of a QCSP frame. The channel is an AWGN with SNR of -10 dB, the residual frequency offset is $f_r = -3.8507 \times 10^{-5}$ and the initial phase is $\phi_0 = 0.5152$. Two different sets of phases can be observed: 1) the phases Ψ_k of wrongly detected CCSK symbols ($d_k \neq c_k$) represented by the shaded red circles. According to (6), those phases are independent with the real phase Θ_k; 2) the phase Ψ_k of correctly detected CCSK symbols ($d_k = c_k$) that are correlated with Θ_k (see gray area in Fig. 2).

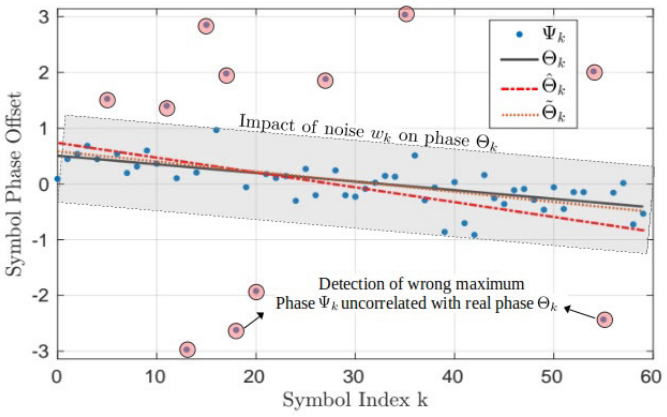

Fig. 2. Phase offsets effect due to the channel Ψ_k, real phase offsets Θ_k, direct method estimation $\hat{\Theta}_k$ and parametric method $\tilde{\Theta}_k$.

In case of wrong decision, the PDF f_ξ of the phase error ξ can be modeled as the PDF of the uniform distribution over the interval $[-\pi, \pi]$, i.e. $f_{\xi_w}(x) = \frac{1}{2\pi}$ for $x \in [-\pi, \pi]$ and 0 otherwise (see Fig. 3.a, .b).

In case of correct decision, the PDF can be closely modeled as the PDF of the normal distribution $N(0, \rho)$; see Fig. 3 (blue curves), where the variance ρ can be numerically calculated. Thus, $f_{\xi_c}(x) = (1/\rho\sqrt{2\pi}) \exp(-\frac{x^2}{2\rho^2})$ [1].

Let us assume that $\mathcal{P}_0$ is the probability of error in the CCSK demodulation. Thus, $f_\xi(x)$ is equal to $f_{\xi_c}(x)$ with a probability of $1 - \mathcal{P}_0$, and it is equal to $f_{\xi_w}(x)$ with a probability $\mathcal{P}_0$, thus, in average,

$$\begin{aligned} f_\xi(x) &= (1 - \mathcal{P}_0) f_{\xi_c} + \mathcal{P}_0 f_{\xi_w} \\ &= \frac{1 - \mathcal{P}_0}{\rho\sqrt{2\pi}} \exp(-\frac{x^2}{2\rho^2}) + \frac{\mathcal{P}_0}{2\pi}, \end{aligned} \tag{8}$$

when $x \in [-\pi, \pi]$, and 0 otherwise. This distribution is shown in Fig. 3-b.

As an empirical verification of the previous theoretical analysis, a Monte Carlo (MC) simulation of 10^6 CCSK symbols c_k at SNR $= -10$ dB has been considered. Fig. 3-a illustrates the experimental phase distribution $f_\xi(x)$ (black curve) as well as its components $(1 - \mathcal{P}_0) f_{\xi_c}$ (blue curve) and $\mathcal{P}_0 f_{\xi_w}$ (red curve). Fig. 3-b illustrates the theoretical counterparts.

[1] Formally, $f_{\xi_c}(x)$ should be defined over $[-\infty + \infty]$; since $\rho < \pi$, $f_{\xi_c}(x)$ will be given at 0 outside $[-\pi, \pi]$ and the required normalization factor is approximated to 1.

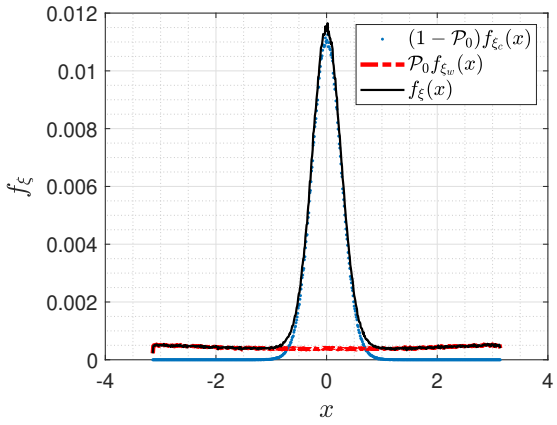

(a) Monte-Carlo

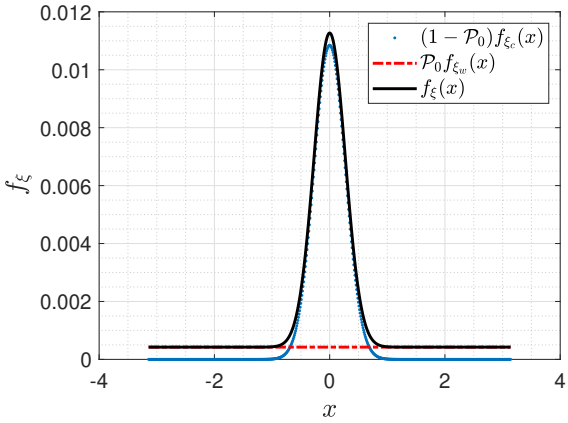

(b) Theoretical

Fig. 3. Distribution of ξ_k at -10 dB where $\mathcal{P}_0 = 0.2375$ and $\rho = 0.32$, (a): MC-simulation, (b): Theoretical.

III. Phase Synchronization with Direct Method

This section discusses the DM to estimate the phase offset of the received frame. According to (3), the vector $\mathbf{\Gamma}$ is a pure sinusoidal vector of length N, with unknown frequency $\omega/(2\pi)$ and an unknown initial phase θ that is corrupted by an AWGN. The estimation of ω and θ is a classical problem of signal processing. First, ω is estimated as $\hat{\omega}$ thanks to the near ML estimator using FFT given in [14]. Then, from the estimated value $\hat{\omega}$, the estimation of the initial phase $\hat{\theta}$ is given as

$$\hat{\theta} = \text{Phase}\left(\sum_{k=0}^{N-1} \gamma_k e^{-j\hat{\omega}k}\right). \tag{9}$$

From $\hat{\omega}$ and $\hat{\theta}$, the phase of the k^{th} symbol is estimated as $\hat{\Theta}_k = \hat{\omega}k + \hat{\theta}$. The values of $\hat{\Theta}_k$, $k = 0, 1, \ldots, N-1$ are shown by the red dashed line in Fig. 2. One can note that, by construction, the difference between the estimated phase $\hat{\Theta}_k$ and the real phase Θ_k is maximized for $k = 0$ and/or $k = N-1$.

The GA of the frequency and initial phase estimation is similar to the DM, except that $\mathbf{\Gamma} = (L_k(d_k))_{k=0,1,\ldots,N-1}$ is replaced by the vector $(L_k(c_k))_{k=0,1,\ldots,N-1}$, i.e., all decisions are assumed to be correct. The GA method gives the optimal estimation $\tilde{\omega}$ and $\tilde{\theta}$ of ω and θ respectively. The corresponding phase for the k^{th} symbol is thus $\tilde{\Theta}_k = \tilde{\omega}k + \tilde{\theta}$.

To compare the performance of the DM with the GA method, 10^4 QCSP frames of length $N = 60$ over GF(64) have been transmitted at an SNR of -10 dB, with each frame affected by a random frequency offset between $[-10^{-3}, 10^{-3}]$ and a random phase offset. For each received frame, ω and θ are estimated based on DM and GA method. Fig. 4.a is a 2D plot where each point shows the phase estimation error corresponding to the final symbol in the received frame $\Theta_{N-1} - \tilde{\Theta}_{N-1}$ as function of the phase estimation error in the first symbol $\Theta_0 - \tilde{\Theta}_0$ of the same frame, calculated based on GA method. Fig. 4.b gives the same result but using the DM method. In both figures, the black circle is the boundary for phase error equals 0.336 radian, which corresponds to an SNR degradation equals to 0.5 dB (i.e. $10\log_{10}(\cos(0.336)^2) = -0.4998$).

The gap in performance between the DM and GA methods is clear, where the former is not reliable and introduces a loss of 0.5 dB (and even more than 1 dB in some cases). The next section shows a novel approach that overcomes this problem and allows to get a performance close to the GA approach.

IV. Parametric Method (PM) for Phase Estimation

This section proposes a new method, named PM, for estimating the phase offset. This method is based on two steps. First, a model of the PDF of each phase error is derived. Then, a ML estimator is applied to find the parameters $(\bar{\omega}, \bar{\theta})$ that the observation "explains the best".

A. ML estimation method

In statistics, after some observed data is given, ML estimation is a method that estimates the parameters of an assumed probability distribution. This is achieved by maximizing a likelihood function so that, under the assumed statistical model, the observed data is the most probable. The point in the parameter space that maximizes the likelihood function is called the ML estimation. In QCSP system, ML estimator can be applied to estimate the frequency and phase parameters $(\bar{\omega}, \bar{\theta})$ of (ω, θ) in (3) as the following

$$(\bar{\omega}, \bar{\theta}) = \arg\max_{\omega,\theta} \Big(\prod_{k=0}^{N-1} f_{\xi_k}(\Psi_k - \omega k - \theta) \Big), \tag{10}$$

where $\Psi_k = \text{Phase}(\gamma_k)$ as defined in (7) and f_{ξ_k} the PDF associated to the phase error of the k^{th} detected symbol. In practice, (10) is evaluated on a discrete 2-dimensional grid, one dimension for $\Theta_0 = \theta$, another for ω. The grid resolution of $\Theta_0 = \theta$ is $\pi/32$, which corresponds to a maximum error of quantization of $\pm\pi/64$, i.e., a maximum of $10\log_{10}(\cos(\pi/64)^2) = 0.01$ dB of SNR degradation. Since θ varies from $-\pi$ to π, the associated grid contains 64 values. For the grid of ω, it is more convenient to specify the final

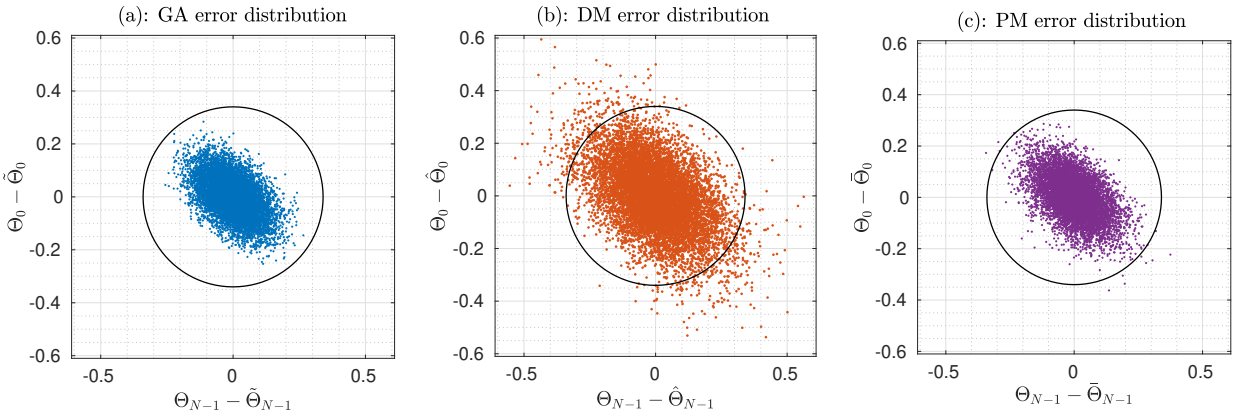

Fig. 4. QCSP phase estimation errors distribution for different methods. The circle corresponds to the boundary of SNR degradation above 0.5 dB.

phase Θ_{N-1}, since $\omega = (\Theta_{N-1} - \Theta_0)/N$ according to (9). In the worst cases, $\theta = +\pi$ (respectively $-\pi$) and $f_r = +10^{-3}$ (respectively, -10^{-3}), leading to the final phase Θ_{N-1} inside the interval $[-\Theta^m, \Theta^m]$ with $\Theta^m = \pi + 2\pi(N-1)qf_r = 8.5\pi$. With the same resolution as Θ_0, the Θ_{N-1} grid contains $(2 \times 8.5) \times 32 = 544$ elements. Altogether, the 2-dimensional grid contains $64 \times 544 = 3.5 \times 10^4$ elements. This very high number can be drastically reduced in practice. For example, it is possible to search the optimal solution with a greedy algorithm stating from the parameters given by the DM.

The quality of the PM thus relies on the quality of the PDFs f_{ξ_k}, $k = 0, 1, \ldots, N-1$ derived in (8). This PDF depends directly on the two parameters: the probability of detection error $\mathcal{P}_0$ and the variance ρ of the phase error of the correct symbol. In the next two sections, we propose first a parametric estimation based on the CCSK decision process. Then the quality of the parameters' estimation is improved by taking the profit of the information computed thanks to the NB-LDPC code.

B. Dependency of f_ξ on CCSK score ratio R

Let s_k be the index of the second-highest decision in (2), i.e.,

$$s_k = \underset{i=0,1,\ldots,q-1, i \neq d_k}{\operatorname{argmax}} \{|L_k(i)|\}, \tag{11}$$

and $\epsilon_k = L_k(s_k)$ its corresponding value. According to [17], the value $|\gamma_k| - |\epsilon_k|$ is related to the reliability of the decision d_k (the higher this value, the higher the reliability of the decision d_k). This difference is normalized by $|gamma_k|$ to make the algorithm insensitive to a scaling factor, thus leading to the relative ratio R_k defined as $R_k = \frac{|\gamma_k| - |\epsilon_k|}{|\gamma_k|}$. For example, $R_k = 0$ means that the decisions d_k and s_k have same reliability, thus d_k is not a reliable decision. On the contrary, R_k close to one indicates a very reliable decision since a high peak exists due to the matched correlation process. This is confirmed by a MC simulation done over 10^8 QCSP frames of length $N = 60$, $q = 64$ at SNR = -10 dB. The probability of error $\mathcal{P}_0$ is estimated as a function of R. As shown in Fig. 5, $\mathcal{P}_0$ decreases from 0.83 when $R = 0$ down to 10^{-5} when R get closed to 0.62. The variance ρ has smaller variation effect when conditioned to R. It decreases from 0.31 when $R = 0$ down to 0.21 for $R = 0.6$.

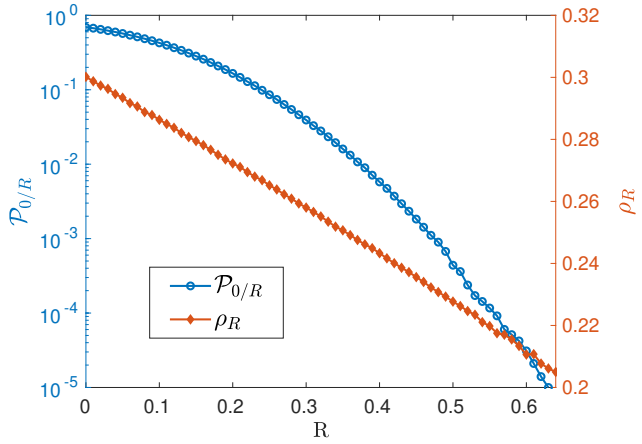

Fig. 5. $\mathcal{P}_{0/R}$ and ρ_R as function of R, at SNR = -10 dB.

In the sequel, $\mathcal{P}_{0/R}(R)$ and $\rho_R(R)$ will denote the PDF parameters values of $f_{\xi/R}$ conditioned to the observed value of R.

C. Dependency of f_ξ on the NB-LDPC code

The probability of error $\mathcal{P}_{0/R}$ can be further enhanced thanks to the information given by the NB-LDPC code, giving a new estimation denoted $\mathcal{P}_{0/R-code}$.

Let us first describe some features of the NB-LDPC code defined by the PCM $\boldsymbol{H}$ of $N-K$ rows and N columns. The code is assumed to be regular, with weights $\mathrm{d}_v = 2$ columns and $\mathrm{d}_c = 3$ rows ($R_c = 1 - 2/3 = 1/3$). Let $\mathcal{M}(j)$ be the set of $\mathrm{d}_c = 3$ variable nodes connected to the j^{th} check node (i.e. the non-null positions of the j^{th} row of $\boldsymbol{H}$) and $\mathcal{N}(i) = \{j_1(i), j_2(i)\}$ the set of $\mathrm{d}_v = 2$ check nodes connected to the i^{th} variable node (i.e. the non-null positions of the i^{th}

column of $\boldsymbol{H}$). The j^{th} Parity Check (PC) equation for a vector $\boldsymbol{D} = (d_0, d_1, \ldots, d_{N-1})$ is defined as

$$\sum_{i \in \mathcal{M}(j)} h(j,i) d_i = 0, \tag{12}$$

where $h(j,i)$ is an element in matrix $\boldsymbol{H}$ at index (j,i).

In the absence of decoding error, $\boldsymbol{D}$ is a codeword and thus, all the PCs are fulfilled. On the other side, if decoding errors exist, some PCs will not be fulfilled. The idea here is to perform one decoding iteration of the code with the hard decision vector $\boldsymbol{D}$. This decoding iteration generates $\mathrm{d}_v = 2$ check to variable messages for each variable node. Let $M_{j_1(i)\to i}$ and $M_{j_2(i)\to i}$ be the two messages sent by the checks $j_1(i)$ and $j_2(i)$ to the variable node i. Those two messages are defined, for $x = 1, 2$, as [18]:

$$M_{j_x(i)\to i} = h(j_x(i), i)^{-1} \sum_{i' \in \mathcal{M}(j_x(i)), i' \neq i} h(j_x(i), i') d_{i'}, \tag{13}$$

where d_i is the intrinsic decision to variable node i.

To lighten notation, index i is omitted, and (M_1, M_2) denote the two check to variable node messages defined in (13). The 3 equality tests $(d = M_1), (d = M_2)$ and $(M_1 = M_2)$ give in total 8 possibilities. This information is used to re-evaluate the reliability of the decision d, and thus, the estimation of the probability of error $\mathcal{P}_{0/R-code}$. For example, when all the equalities are fulfilled, the local decision is consistent with the code structure and $\mathcal{P}_{0/R-code}$ becomes very low. On the contrary, when $(d \neq M_1), (d \neq M_2)$ and $(M_1 = M_2)$, the local decision is inconsistent with the code structure and $\mathcal{P}_{0/R-code}$ increases. The exact mathematical determination of $\mathcal{P}_{0/R-code}$ as a function of R and the equality test results are not presented due to the lack of space. Fig. 6 shows examples of PDF $f_{\xi/R-code}$ for several values of parameters R and equality test results. We can figure out that probability of having error close to zero is higher when R is increased and the equality tests are satisfied.

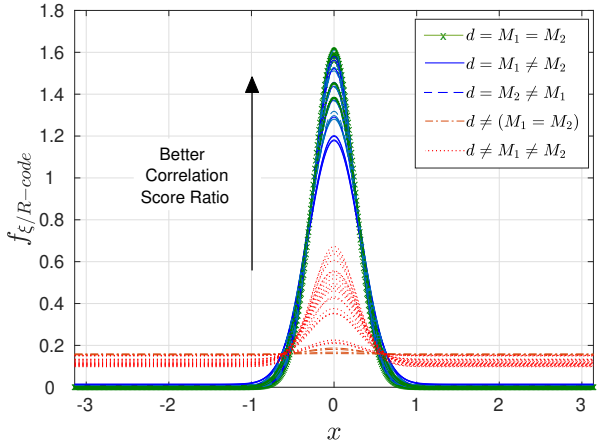

Fig. 6. $f_{\xi/R-code}$ depending on the CCSK ratio R and Code-information, at SNR = -10 dB.

This conditioned PDF $f_{\xi/R-code}$ is used to determine the parameters $(\bar{\omega}, \bar{\theta})$ in (10). Values of $\bar{\Theta}_k,\ k = 0, 1, \ldots, N-1$ are shown as an example by the brown dotted line in Fig. 2. Also, Fig. 4-c shows the distribution of the phase offset errors $\bar{\xi}_k$, using the PM phase estimator, for $k = 0$ and $k = N - 1$ after transmitting 10^4 QCSP frames in an AWGN channel of SNR = -10 dB and random phase offsets. We can figure out that PM aided by the information of the QCSP frame approaches the GA method.

V. Simulation Results

This section presents the simulation results of the FEC probability of error for a QCSP received frame, of $N = 60$ symbols, exposed to random phase offsets. This is implemented using the different phase synchronization scenarios (no phase synchronization, DM, PM) and the ideal case of FEC where the frame has no phase offset. The MC simulations are run over an AWGN channel with stopping criteria of 100 miss-corrected frames, NB-LDPC encoder with coding rate $R_c = 1/3$, $q = 64$, initial phase offset randomly distributed in $[-\pi, \pi]$, and frequency shifts considered to be uniform randomly-distributed in the boundary of $\pm 10^{-3}$. Moreover, the GF(64)-LDPC decoder defined in [19] is implemented using the Extended Mean Sum (EMS) algorithm with 30 decoding iterations and $n_m = 20$ [20]. We can see that a NB-LDPC decoder clearly looses its good performance when not caring about the phase offset, and looses up to 0.5 dB when using the DM. However, when using the proposed PM phase estimator (the blue curve) approximately maintains the same performance of the FEC $\mathcal{P}_\epsilon$ as when no phase offset does exist.

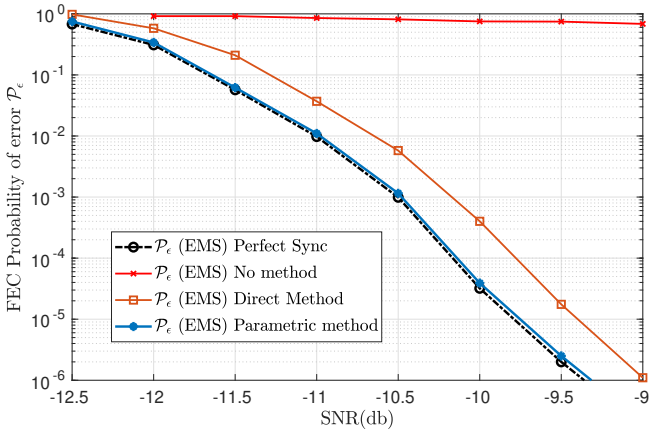

Fig. 7. FEC with different scenarios.

VI. Conclusion

The paper presented a phase synchronization algorithm for QCSP frames operating at very low SNR (-10 dB) that can help in maintaining the FEC performance as if phase offset is not existing. The proposed PM mitigates the phase ambiguity based on the ML method aided by two side information

from the QCSP structure. The first information is from the CCSK demodulation score ratios, where the ML method used a weighted version by privileging the symbols received with high reliability. The second information is from the NB-LDPC code properties, thanks to the code structure.

This work will be extended in several directions in the near future. First, a performance-complexity trade-off will be studied. Then, performance assessment at different frame lengths, code rates, and GF(q) will be addressed. Finally, the different scenarios of simulations considered over an AWGN channel will be run over the Rayleigh fading channel.

REFERENCES

[1] Shafique, Kinza and Khawaja, Bilal A. and Sabir, Farah and Qazi, Sameer and Mustaqim, Muhammad, "Internet of Things (IoT) for Next-Generation Smart Systems: A Review of Current Challenges, Future Trends and Prospects for Emerging 5G-IoT Scenarios," *IEEE Access*, vol. 8, pp. 23 022–23 040, 2020.

[2] B. Lee, S. Park, D. J. Love, H. Ji, and B. Shim, "Packet structure and receiver design for low latency wireless communications with ultra-short packets," *IEEE Transactions on Communications*, vol. 66, no. 2, pp. 796–807, 2018.

[3] Rahbari, Hanif and Krunz, Marwan, "Exploiting Frame Preamble Waveforms to Support New Physical-Layer Functions in OFDM-Based 802.11 Systems," *IEEE Transactions on Wireless Communications*, vol. 16, no. 6, pp. 3775–3786, 2017.

[4] Y. Polyanskiy, "Asynchronous Communication: Exact Synchronization, Universality, and Dispersion," *IEEE Transactions on Information Theory*, vol. 59, no. 3, pp. 1256–1270, March 2013.

[5] A. Azari, P. Popovski, G. Miao, and C. Stefanovic, "Grant-Free Radio Access for Short-Packet Communications over 5G Networks," in *GLOBECOM 2017 - 2017 IEEE Global Communications Conference*, 2017, pp. 1–7.

[6] B. Bloessl and F. Dressler, "mSync: Physical Layer Frame Synchronization Without Preamble Symbols," *IEEE Transactions on Mobile Computing*, vol. PP, pp. 1–1, 02 2018.

[7] P. Walk, P. Jung, B. Hassibi, and H. Jafarkhani, "MOCZ for Blind Short-Packet Communication: Practical Aspects," *IEEE Transactions on Wireless Communications*, vol. 19, no. 10, pp. 6675–6692, 2020.

[8] Y. Rahamim, A. Freedman, and A. Reichman, "Methods for carrier synchronization of short packet turbo coded signals," in *2004 IEEE 15th International Symposium on Personal, Indoor and Mobile Radio Communications (IEEE Cat. No.04TH8754)*, vol. 3, 2004, pp. 1983–1987 Vol.3.

[9] K. Saied, A. C. A. Ghouwayel, and E. Boutillon, "Short frame transmission at very low snr by associating ccsk modulation with nb-code," *IEEE Transactions on Wireless Communications*, pp. 1–1, 2022.

[10] G. M. Dillard, M. Reuter, J. Zeiddler, and B. Zeidler, "Cyclic code shift keying: a low probability of intercept communication technique," *IEEE Transactions on Aerospace and Electronic Systems*, vol. 39, no. 3, pp. 786–798, July 2003.

[11] O. Abassi, L. Conde-Canencia, M. Mansour, and E. Boutillon, "Non-binary coded CCSK and Frequency-Domain Equalization with simplified LLR generation," in *2013 IEEE 24th Annual International Symposium on Personal, Indoor, and Mobile Radio Communications (PIMRC)*, Sep. 2013, pp. 1478–1483.

[12] C. Monière, K. Saied, B. Legal, and E. Boutillon, "Time sliding window for the detection of CCSK frames," in *the IEEE Workshop on Signal Processing Systems (SiPS'2021)*, Oct. 2021, pp. 1–6.

[13] K. Saied, A. Al Ghouwayel, and E. Boutillon, "Blind Time-Synchronization of CCSK Short Frames," in *The 17th International Conference on Wireless and Mobile Computing, Networking and Communications (WiMob21)*, Oct. 2021, pp. 1–6.

[14] M. Fitz, "Further results in the fast estimation of a single frequency," *IEEE Transactions on Communications*, vol. 42, no. 234, pp. 862–864, 1994.

[15] E. Boutillon. "PN Sequence Generation in QCSP systems". [Online]. Available: https://qcsp.univ-ubs.fr/wp-content/uploads/2021/11/Sequence_PN.pdf

[16] O. Abassi, L. Conde-Canencia, M. Mansour, and E. Boutillon, "Non-Binary Low-Density Parity-Check coded Cyclic Code-Shift Keying," in *2013 IEEE Wireless Communications and Networking Conference (WCNC)*, 2013, pp. 3890–3894.

[17] C. Marchand and E. Boutillon, "Nb-ldpc check node with pre-sorted input," in *2016 9th International Symposium on Turbo Codes and Iterative Information Processing (ISTC)*, 2016, pp. 196–200.

[18] X. Zhang, F. Cai, and S. Lin, "Low-Complexity Reliability-Based Message-Passing Decoder Architectures for Non-Binary LDPC Codes," *IEEE Transactions on Very Large Scale Integration (VLSI) Systems*, vol. 20, no. 11, pp. 1938–1950, 2012.

[19] (2020) Web site on Non-Binary LDPC. [Online]. http://www-labsticc.univ-ubs.fr/nb-ldpc/.

[20] E. Boutillon, L. Conde-Canencia, and A. Al Ghouwayel, "Design of a GF(64)-LDPC Decoder Based on the EMS Algorithm," *IEEE Transactions on Circuits and Systems I: Regular Papers*, vol. 60, no. 10, pp. 2644–2656, Oct 2013.